Plant Physiol. (1997) 113: 895–901

Photosynthetic Electron Transport in Single Guard Cells as Measured by Scanning Electrochemical Microscopy[1]

Michael Tsionsky, Zoe G. Cardon, Allen J. Bard, and Robert B. Jackson*

Department of Chemistry and Biochemistry (M.T., A.J.B.) and Department of Botany (R.B.J.), University of Texas, Austin, Texas 78712; and Department of Biology, Bowdoin College, Brunswick, Maine 04011 (Z.G.C.)

Scanning electrochemical microscopy (SECM) is a powerful new tool for studying chemical and biological processes. It records changes in faradaic current as a microelectrode (≤7 μm in diameter) is moved across the surface of a sample. The current varies as a function of both distance from the surface and the surface's chemical and electrical properties. We used SECM to examine in vivo topography and photosynthetic electron transport of individual guard cells in *Tradescantia fluminensis*, to our knowledge the first such analysis for an intact plant. We measured surface topography at the micrometer level and concentration profiles of O_2 evolved in photosynthetic electron transport. Comparison of topography and oxygen profiles above single stomatal complexes clearly showed photosynthetic electron transport in guard cells, as indicated by induction of O_2 evolution by photosynthetically active radiation. SECM is unique in its ability to measure topography and chemical fluxes, combining some of the attributes of patch clamping with scanning tunneling microscopy. In this paper we suggest several questions in plant physiology that it might address.

SECM, a type of scanning probe microscopy, was introduced in 1989 as a technique to study processes occurring on chemical interfaces (Bard et al., 1989). SECM is a "chemical microscope" that operates in two modes, feedback and collection (see "Materials and Methods"). The feedback mode provides three-dimensional surface topography, with the current in the microelectrode varying with distance from the sample surface (Bard et al., 1991). The collection mode records chemical changes at the surface, including which sample regions are insulating or conducting, and the rate of generation of an electrochemical agent (in our case, O_2 evolved in photosynthetic electron transport). Since 1989 a variety of complex electrochemical and catalytic reactions have been studied, including surface topography and chemical reactions for metals, semiconductors, polymers, and liquid/liquid interfaces (e.g. Mirkin et al., 1992; Horrocks et al., 1994; Wei and Bard, 1995).

SECM is related to a variety of SPTs, including STM, in which surface topography is obtained by recording the tunneling current between electrode and sample, and atomic force microscopy, which measures the force between electrode and sample for a given x-y position over the surface (Hansma et al., 1989). Just as in STM, the microelectrode in SECM is controlled with nanometer resolution in the x, y, and z directions (Bard et al., 1991). The main advantage of SECM compared with other SPTs is that it provides not just topographic information at micrometer and submicrometer scales, but also information about the concentration of electroactive species above the probed surface (Lee et al., 1990). This combination of topographic and electrochemical information is also one way that SECM differs from typical patch-clamp techniques, which provide no topographical data. Although the resolution of SECM is 100 nm under some conditions, it does not yet provide the atomic resolution of STM or atomic force microscopy. SECM resolution is improving rapidly and is already sufficient for us to examine such a biological phenomenon as O_2 diffusion from individual stomata in intact leaves.

Stomata act as valves on the surface of leaves, balancing CO_2 availability for photosynthesis with water loss to the atmosphere. Over the last century instruments ranging from rudimentary porometers to complex gas-exchange systems have been used to investigate stomata from the perspective of whole-leaf or whole-plant physiology (e.g. Sestak et al., 1971; Zeiger et al., 1987; Jackson et al., 1991). Investigations at the cellular level, in turn, have attempted to understand the mechanisms by which guard cells respond to their environment, most often using epidermal peels or guard cell protoplasts (for reviews, see MacRobbie, 1987; Assmann, 1993). Peels and protoplasts, however, may not always reflect in vivo, unstressed physiology. Guard cells isolated from subsidiary cells (either physically in a protoplast preparation or via cell death during peeling) no longer communicate with a live, turgid epidermis that provides back-pressure against stomatal turgor. Isolated guard cells also have been separated from ion sources and sinks fundamental for guard cell function in vivo. Ideally, experiments with functionally or physically isolated guard cells should be tested in intact leaves, and observations of stomatal behavior at the physiological level must be linked with cell-level processes.

[1] Support was provided by the National Science Foundation, the Welch Foundation, and the Andrew W. Mellon Foundation. Z.G.C. was supported by a Department of Energy Distinguished Postdoctoral Fellowship for Global Change.

* Corresponding author; e-mail rjackson@mail.utexas.edu; fax 1–512–471–3878.

Abbreviations: E, electric potential; i_T, steady-state tip current; $i_{T,\infty}$, steady-state tip current far from the sample surface; SECM, scanning electrochemical microscopy; SPT, scanning probe techniques; STM, scanning tunneling microscopy; UME, ultra microelectrode.

One limitation is the lack of techniques for probing chemical processes at the cellular level while the cell is living and functioning in its normal environment. The development of patch-clamping has led to the characterization of many ion channels and signaling systems in guard cell protoplasts (e.g. Assmann, 1993), although the behavior and chemistry of isolated guard cells may sometimes differ from that of intact leaves. Chlorophyll fluorescence provides one avenue for probing photosynthetic activity in living guard cells in epidermal peels and protoplasts (e.g. Melis and Zeiger, 1982; Shimazaki, 1989), and the technique has also been applied to guard cells in intact leaves (Cardon and Berry, 1992). Another recent approach examines guard cell membranes in epidermal peels that are patch-clamped through laser-cut holes in cell walls (Henriksen et al., 1996).

In this paper, we present SECM as a new technique for observing guard cell chemistry and leaf surface topology in vivo, and as a new tool for physiologists in general. Understanding the role of guard cell chloroplasts in stomatal functioning is critically important, yet controversy still exists regarding the activity of guard cell chloroplasts and their energetic contribution to ion uptake and stomatal opening (Shimazaki, 1989; Reckmann et al., 1990; Gautier et al., 1991; Wu and Assmann, 1993). We first provide a description of SECM, including its modes of operation and the information to be gained in each mode. We then apply SECM to photosynthetic electron transport and topography in variegated leaves of *Tradescantia fluminensis*, which is ideal for photosynthetic studies because its leaves provide both green regions, where chloroplasts are present in mesophyll and guard cells, and white regions, where chloroplasts are present only in the guard cells (Cardon and Berry, 1992). We use SECM to examine topography and net photosynthesis in the green leaf regions (as measured by O_2 evolution). Finally, as a more challenging application of SECM, we demonstrate in vivo photosynthetic electron transport for individual guard cells in white leaf regions.

MATERIALS AND METHODS

SECM

SECM is based on the steady-state current or E detected by the SECM UME. The UME tip for measuring current is usually made of a single metal (e.g. Au or Pt) wire or carbon fiber sealed into an insulating material (e.g. glass, wax, or epoxy resin). Only the wire cross-section is exposed in the solution. As in most SPTs, the resolution of SECM increases as the tip diameter decreases. There are two operational modes of SECM. The feedback mode is used mainly to obtain topographic images, and the collection mode provides concentration profiles of an electroactive species across the sample surface.

The feedback mode of SECM is based on the effect of an oxidized electroactive substrate (O), $O + e^- \rightarrow R$, on UME current. Because of fast hemispherical diffusion of the electroactive species to the UME surface, the i_T is well defined and relatively unaffected by convection (Bard and Faulkner, 1980). $i_{T,\infty}$ is calculated as:

$$i_{T,\infty} = 4nFC_oDa \quad (1)$$

where n is the number of electrons, F is the Faraday constant, D is the diffusion coefficient of species O, C_o is the concentration of species O in the bulk solution, and a is the radius of the tip UME. When the UME is placed sufficiently close to the insulative substrate (e.g. of the order of the tip radius), i_T decreases relative to $i_{T,\infty}$ because the insulative substrate partially blocks diffusion of O to the UME. The closer the tip is to the substrate, the greater the reduction in current. In the ideal case (i.e. the tip UME and substrate are smooth and parallel to each other), UME current should approach zero as the separation distance approaches zero. Although Equation 1 is most appropriate for microelectrodes with a glass radius at least 10 times the electrode radius, such microelectrodes are unwieldy for fine-scale work over a rough surface. Our glass radius was two to three times larger than the electrode radius. Such electrodes generally deviate from Equation 1 by less than 10%, and our measurements showed almost perfect agreement (see "Results").

The dependence of tip current on distance to the insulative surface (d) is given by the following equation (Mirkin et al., 1992):

$$\frac{i_T}{i_{T,\infty}} = (0.292 + [1.5151/L] + 0.6553e^{[-2.4035/L]})^{-1} \quad (2)$$

where L is the normalized distance between the tip UME and the substrate ($L = d/a$). In feedback mode as the tip travels across an insulative surface increases in current represent hollows and decreases in current represent humps (i.e. negative feedback).

In collection mode the UME detects a species generated on or diffusing from the substrate. UME response can represent current or potential. If the substrate generates an electroactive species that can be detected by the UME, UME current will increase as the tip approaches. However, while operating in collection mode the tip-substrate distance cannot be calculated definitively because the tip response is a function of both the substrate activity and the tip-substrate separation. In the case where the substrate is an insulator and has isolated regions that generate an electroactive species (in our case, O_2 evolution from a leaf), the image of such a surface can be obtained by scanning the UME across the substrate. Regions of active evolution will yield greater tip response compared with the rest of the insulative or inactive surface.

The SECM used in our experiments (Fig. 1) was described by Wipf and Bard (1991). Briefly, a UME was mounted on an XYZ stage (Burleigh Instruments, Fishers, NY) and was biased at a potential of oxygen reduction using an E-400 potentiostat. Nanometer control of the UME in x, y, and z directions by attached piezoelectric elements was provided by a CE-1000 controller and personal computer (Inchworm Controller, Burleigh Instruments). Data were acquired using unpublished software of D.O. Wipf.

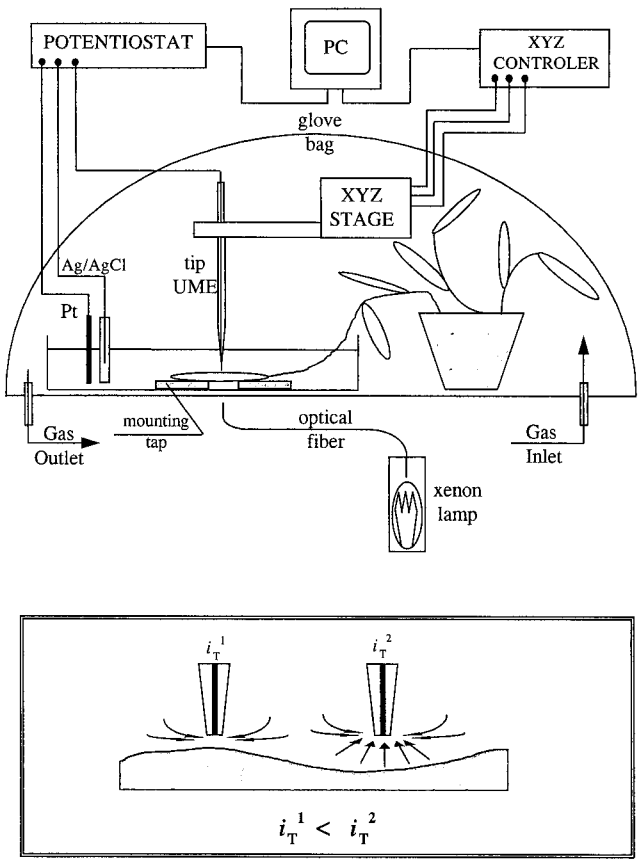

Figure 1. SECM apparatus for in vivo experiments of leaf surfaces. The upper panel describes the experimental station, and the lower panel illustrates how topography affects diffusion of a substrate to the UME tip.

The SECM UMEs were prepared as described by Bard et al. (1989) with the following modifications. The UME used for the experiments was a 7-μm-diameter C fiber (Goodfellow Corp., Berwyn, PA) that was heat-sealed in a 3-mm o.d. glass capillary drawn down and polished until the wire cross-section was exposed. The counter and reference electrodes attached to the potentiostat (Fig. 1) were a 0.5-mm-diameter Pt wire and a Ag/AgCl wire, respectively, immersed in saturated KCl. All reported values of E are given relative to the Ag/AgCl reference electrode. All of the experiments were performed in a 0.1 M buffer solution (prepared from $NH_4H_2PO_4$ and $[NH_4]_2HPO_4$ in deionized water [Milli-Q, Millipore]) at pH 7.0. A xenon lamp with an attached optical fiber (1 mm in diameter) provided the PAR source for photosynthesis in the SECM. Light intensity was measured with a quantum sensor (Li-Cor, Lincoln, NE) and was maintained between 700 and 800 μmol m^{-2} s^{-1} for all experiments.

Description of Plants and Experiments

Tradescantia fluminensis Variegata clones were grown in a walk-in growth chamber with a photon flux density of 350 μmol m^{-2} s^{-1} and a 13-h photoperiod. The day and night temperatures were 24 and 20°C, respectively. Each plant was grown in a 2-L pot with Metromix 700 potting medium (Scotts Co., Marysville, OH). Plants were watered daily to excess and fertilized weekly with approximately 0.1 L of 40 mM $NH_4H_2PO_4$, 25 mM CH_4N_2O, and 14 mM K_2O (plus trace elements).

Prior to SECM experiments, *T. fluminensis* leaves were carefully washed with deionized water. The hypostomatous leaves were held between two soft O-rings or with mounting tape. In all of the experiments the leaves were alive and remained attached to the plant. When the UME scans an illuminated portion of leaf, the tip responds to a combination of leaf topography and O_2 availability. The large background concentration of O_2 in air (and in air-saturated solution) makes the potential detection of photosynthetically derived O_2 more difficult, particularly in a white region of the leaf, where chloroplasts are present only in the guard cells. To maximize the resolution for detecting O_2 generated in photosynthetic electron transport, two of the images were generated by placing the plant and experimental apparatus into a glove-bag for short periods of time with reduced atmospheric O_2 (approximately 2% by volume).

To obtain images of leaf topography, the tip UME was brought to <10 μm from the leaf surface in the dark. The tip was moved in the y direction at a speed of 10 μm/s while collecting i_T. After finishing one pass (usually 100–250 μm), the tip was shifted 5 to 10 μm in the x direction and then returned in the opposite y direction. The time required to obtain a square image of 200 × 200 μm was 10 to 20 min. If desired, a series of stable, reproducible images of the same leaf area could be obtained sequentially over several hours, depending on suitable control of leaf conditions. To map the topography of open stomata in the absence of O_2 generated by photosynthesis, 0.1 M KCl (Humble and Hsiao, 1969) was used to open stomates in one image. For all images taken directly over a stomatal complex, the location of the complex was first detected by topographic scan before any O_2 measurements were taken.

In addition to examining topography and O_2 evolution across the surface of the leaf, we also examined the response of specific white and green positions on the leaf to a step change in light availability (from 800 μE m^{-2} s^{-1}, to dark, and back to 800 μE m^{-2} s^{-1}). For these experiments (Figs. 6B and 7B), the UME tip was positioned directly above an illuminated stomatal complex until i_T reached a steady maximum. The light was then switched off for 5 to 10 min, after which PAR was restored to 800 μE m^{-2} s^{-1}. i_T was monitored continuously throughout the changes in illumination. This fixed-tip approach was used because stomatal aperture can change rapidly over the 10 to 20 min required to image a 200- × 200-μm leaf region after a change in PAR. Focusing on individual stomata yielded much more precise results.

RESULTS

Typical steady-state voltammograms (graphs of i_T versus E) in buffer saturated with 21, 10, and 2% O_2 show the sensitivity of the UME to O_2 (Fig. 2). During SECM experiments the tip UME was biased at a potential of −0.95 V, at

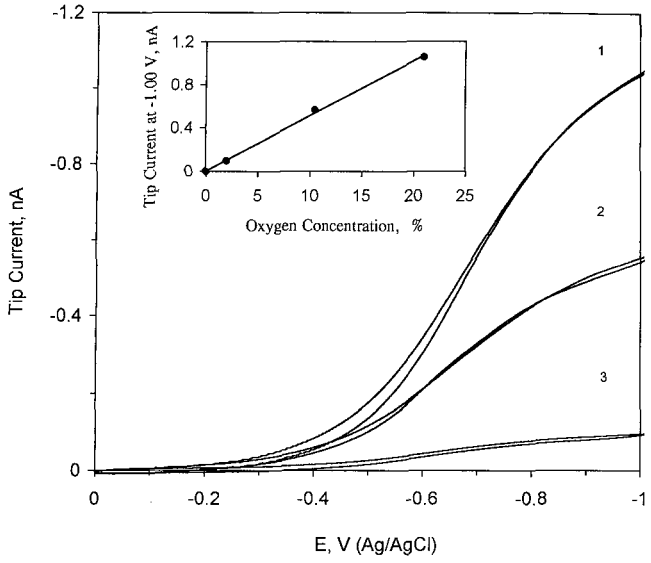

Figure 2. Typical cyclic voltammograms (i_T versus E) for the reduction of dissolved O_2 measured with a 7-μm-diameter carbon UME tip in ammonium buffer solution (pH 7.0). Curve 1 corresponds to an air-saturated solution (79% N_2, 21% O_2), curve 2 to a solution saturated in 90% N_2 and 10% O_2, and curve 3 to a solution saturated in 98% N_2 and 2% O_2. i_T initially increases with applied potential (E) for all curves, eventually becoming independent of potential but linearly dependent on O_2 concentration. The pair of curves for each O_2 concentration represent the two cases of ascending and descending E.

which level voltammograms show well-defined, diffusion-limiting current for dissolved oxygen reduction that is relatively independent of potential but linearly dependent on O_2 concentration (Fig. 2).

The ability of the UME to detect O_2 generated in photosynthesis above an individual stomatal complex is shown clearly by graphing i_T versus the distance between the UME tip and the leaf (Fig. 3A). Curves 1 and 2 were both generated in an air-saturated solution, but were generated in the dark and light, respectively (Fig. 3A). In the dark (without photosynthesis and with stomates closed), i_T decreased as the UME tip approached the leaf surface, in precise agreement with SECM theory for an insulative substrate in negative feedback (Fig. 3A, curve 1; solid line generated from Eq. 2). In the presence of PAR, however, normalized i_T was constant until approximately 10 μm distance from the leaf, below which it increased in response to photosynthetically generated O_2 diffusing through the stomate (Fig. 3A, curve 2). Figure 3B (curve 1) shows the identical theoretical line presented in Figure 3A, but at an expanded scale of distance. If a previously illuminated leaf is placed in the dark and quickly examined with the SECM, normalized i_T does not immediately follow SECM theory for an insulative substrate (Fig. 3B, curve 2). This results from residual O_2 evolution/diffusion from the leaf to the solution. After a short time, an equilibrium is reached and the leaf surface begins to show pure insulative behavior (Fig. 3B, curve 2 converges to curve 1).

To present the physical structure of the stomatal complex in *T. fluminensis*, a scanning electron microscopy image of such a complex is presented in Figure 4. The guard cells are approximately 40 μm in length (the reference bar is 20 μm long). A topographic image by SECM of a 200- × 200-μm leaf area shows three stomatal complexes (Fig. 5). Prior to making the image, the stomates were opened by applying 0.1 M KCl, and SECM clearly detects the open stomatal pores. Because the SECM was operating in negative-feedback mode, the image in Figure 5A is inverted (i.e. the dark areas represent bulges on the leaf surface and correspond to low i_T). This inverted image can be converted to the proper physical orientation by Equation 2 (Fig. 5B). As measured with SECM, a typical *T. fluminensis* stomatal complex protrudes approximately 4 μm from the surrounding epidermal region of the leaf.

In addition to purely topographic images, SECM can be used to monitor O_2 evolution from an illuminated leaf for an individual stomate or leaf region. Such a 200- × 200-μm region of a green leaf shows three peaks in i_T corresponding to O_2 evolution from three stomata (Fig. 6A). i_T values for these peaks are at least twice background i_T for the leaf

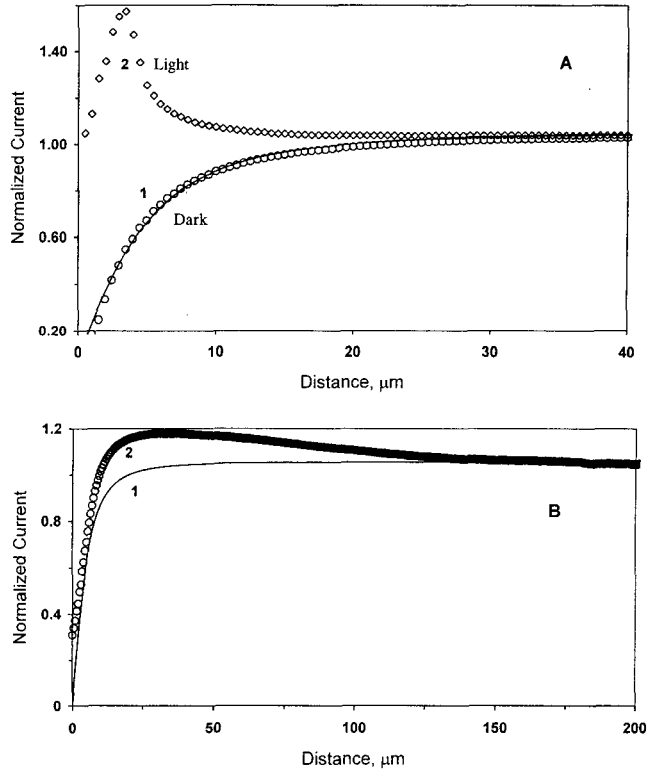

Figure 3. Normalized i_T as a function of distance to the surface of a green leaf maintained in the dark (A, curve 1) and in the light (A, curve 2). Curve 1 (A) was generated by moving the UME tip toward the stomate of a leaf immersed in air-saturated solution and in darkness for 20 min. Curve 2 (A) is for an illuminated leaf in solution saturated with low O_2 (air with 2% O_2). The solid "line" in both panels is the theoretical path for the approach of a tip to an insulative surface (generated from Eq. 2). i_T for a leaf maintained in the dark matches the theoretical path almost perfectly in the absence of O_2 evolution (A, curve 1). B, Curve 2 shows the approach of the UME tip for a leaf recently placed in the dark. Because of residual O_2 diffusion, the leaf does not yet act as a perfect insulator. All measurements were made with a 7-μm-diameter carbon microelectrode.

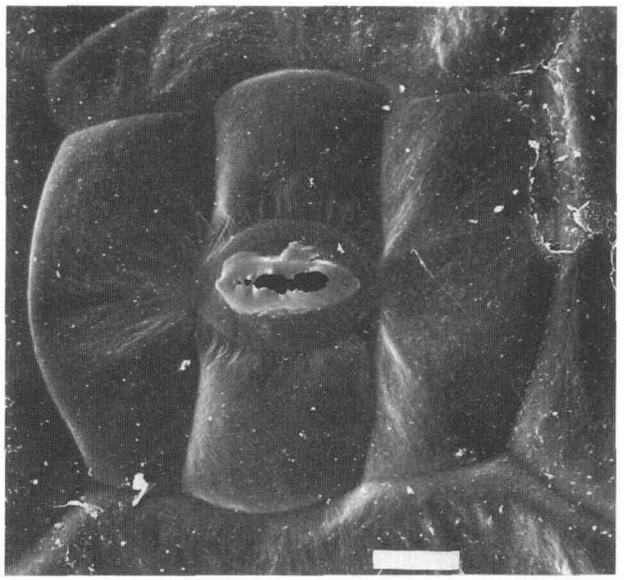

Figure 4. Scanning electron microscopy image of a stomatal complex of *T. fluminensis*. Bar = 20 μm.

surface as a whole. Figure 6A cannot be inverted into a strictly topographic image because i_T reflects both topography and O_2 evolution, so to contrast images of a leaf in the light and dark, Figure 6A should be compared with Figure 5A.

If the UME tip is held in position above an individual stomate, the response to changes in PAR can be examined. When the light source is eliminated, i_T decreases as O_2 evolution from the stomate slows (Fig. 6B). The signal does not completely disappear, because of residual diffusion of O_2 into the solution and because the solution maintains a minimum equilibrium O_2 concentration. When the PAR is restored, i_T increases as photosynthesis and O_2 evolution recommence (Fig. 6B).

Having demonstrated the usefulness of SECM for topography and for O_2 evolution in a green leaf, we then examined in vivo photosynthetic electron transport in guard cells of a white leaf region, in which functional, green chloroplasts are present only in the guard cells. An SECM image of such a region is presented in Figure 7A. The stomatal complex is visible as a ring-shaped structure with a peak in the center due to O_2 evolution. Additional evidence for photosynthetic electron transport in guard cells is provided by manipulating PAR while holding the UME tip above an individual stomate. When the light source is eliminated, i_T decreases as O_2 evolution from the guard cells slows (Fig. 7B). The signal does not decrease (or increase) as quickly as in Figure 6B because the O_2 signal is much smaller in the white portion of the leaf than in the green. When PAR is restored, a detectable increase in i_T and O_2 evolution is visible beginning approximately 2 min after restoration of the light (Fig. 7B).

DISCUSSION

There are two kinds of electrode probes used in SECM. The most convenient are voltammetric electrodes, in which an electrochemical reaction can be driven and a resulting current is measured. The O_2 electrode is this type of probe, with O_2 reduced to H_2O_2 at a carbon electrode. Voltammetric electrodes are used to measure other species that can undergo oxidation or reduction (e.g. hydroquinone, ascorbic acid, dopamine, etc.). The second type of electrode is the potentiometric probe (Arca et al., 1994), which is similar to a specific ion electrode, in which the potential responds to the concentration (activity) of a particular species. Potentiometric probes can be made for H^+, K^+, and NH_4^+, as just a few examples.

For most photosynthetic studies, measuring CO_2 uptake is more desirable than measuring O_2 evolution due to the lower background signature of CO_2 in air (350 versus 210,000 μL L^{-1} for CO_2 and O_2, respectively). Unfortunately, there is not yet a convenient method in SECM to monitor CO_2 evolution from chemical or biological substrates. Measurements of CO_2 are possible through changes in solution pH, although the method is not as accurate as

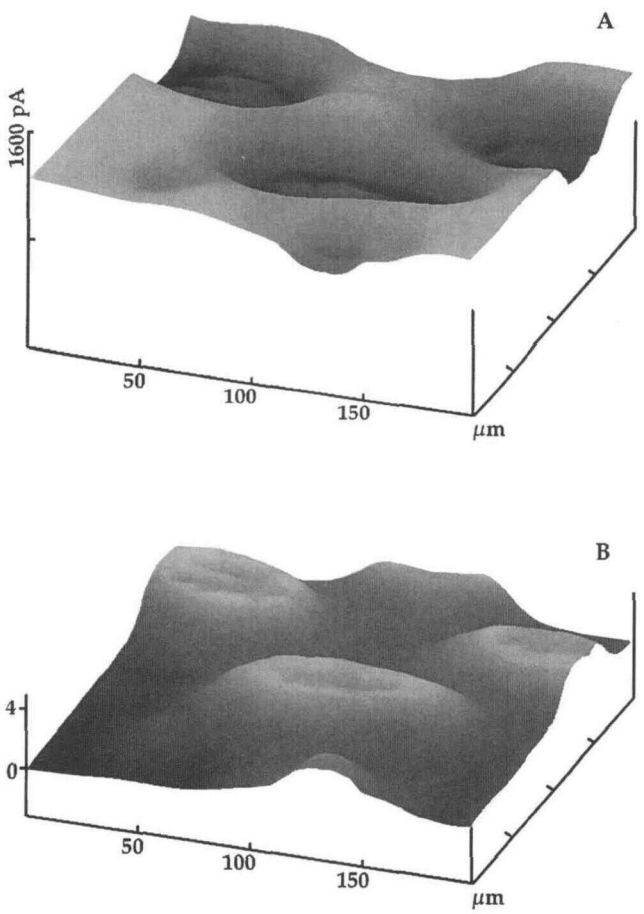

Figure 5. SECM images of a green portion of the leaf obtained with a 7-μm-diameter carbon tip in an air-saturated solution in the dark. A, i_T across the leaf surface. Because the data were generated in negative-feedback mode, the image is inverted (i.e. the dark areas represent bulges on the surface and correspond to low i_T). B, The image in A returned to the proper physical orientation (y axis in μm). The images were obtained 30 min after addition of 0.1 M KCl to the buffer solution to open stomates.

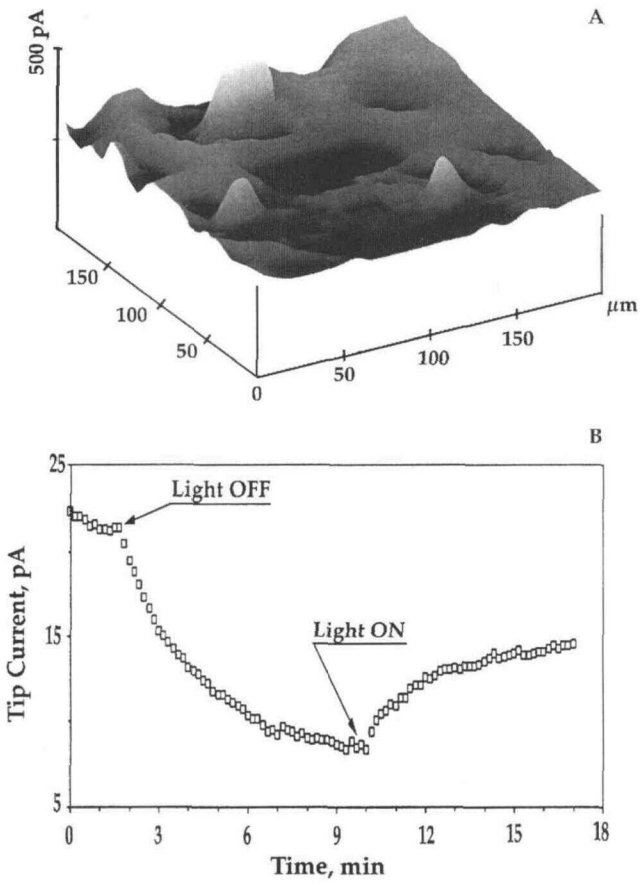

Figure 6. A, O_2 evolution from three stomata of an illuminated green leaf region (200 × 200 μm). The *x* and *y* axes represent position on the leaf; the *z* axis is i_T measured in feedback mode. B, The response of i_T to step changes in light availability when held over a stomate in a green leaf region. Measured current tracks O_2 diffusion and decreases after the leaf is placed in the dark and increases after reillumination (800 μE m^{-2} s^{-1}). Measurements for A and B were made with a 7-μm-diameter carbon microelectrode.

the various electrodes described above. For this reason we monitored O_2 evolution in *T. fluminensis* in part by lowering background O_2 levels for short periods of time in a glove-bag. By this method we were able to obtain sufficient resolution to examine photosynthetic electron transport of individual guard cells in the white regions of *T. fluminensis* leaves. To make certain that the O_2 detected in the white leaf regions was derived solely from guard cells, we used fluorescence microscopy to compare white and green leaf regions. Fluorescence microscopy confirmed the lack of chlorophyll in mesophyll cells for the white leaf regions (R.B. Jackson, unpublished data).

The ability of SECM to detect extremely small fluxes of O_2 evolved from photosynthetic electron transport in individual guard cells is a striking example of the sensitivity of SECM in examining biological systems. During recent decades, a number of papers confirmed the existence of PSI, PSII, and cyclic and noncyclic photosynthetic electron transport in thylakoids of stomatal guard cells (e.g. Dyar, 1953; Outlaw et al., 1981), although the existence and function of Calvin cycle enzymes remains controversial. Some of these studies and the techniques used include (a) fluorescence techniques to examine electron transport (e.g. Zeiger et al., 1980), (b) DCMU to block red-light-induced O_2 production (Shimazaki et al., 1982), (c) A_{518} to probe thylakoid energization and photophosphorylation (Grantz et al., 1985), and (d) direct measurement of red-light-induced O_2 evolution in solution containing guard cell protoplasts (Shimazaki and Zeiger, 1987). All of these studies, however, were conducted with epidermal peels, isolated protoplasts, or isolated chloroplasts. SECM provides the means to measure the extremely small fluxes of O_2 (in this case) or ions at the cellular level in intact living plants.

There are a number of fruitful areas of research to be pursued with SECM, particularly when combined with biochemical analyses. The examination of ion fluxes associated with stomatal response to light is one obvious possibility. Using enzymatic techniques (e.g. Morris et al., 1981), it should be possible to access both guard and sub-

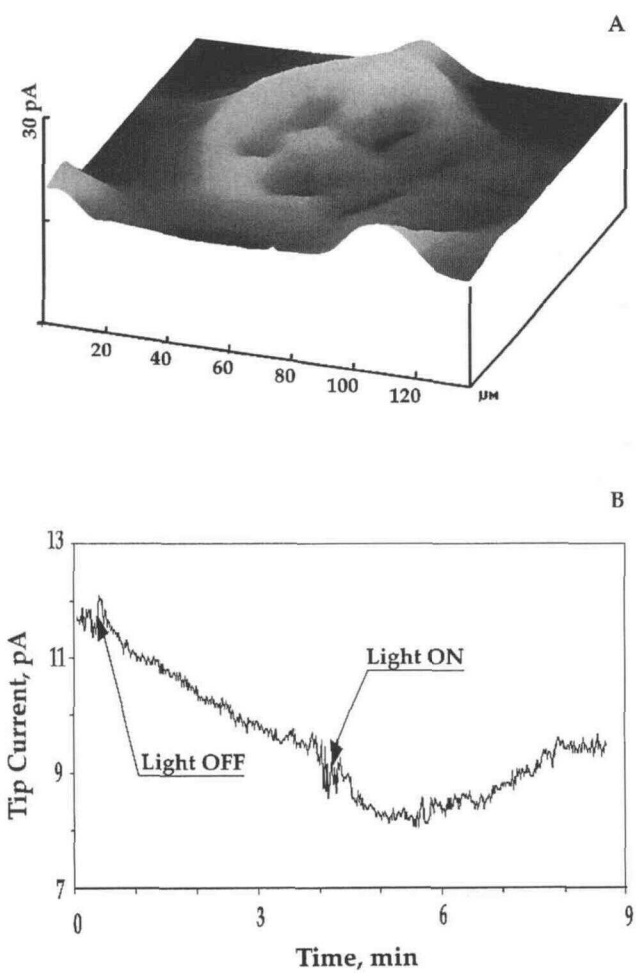

Figure 7. A, A single, illuminated stomatal complex in a white leaf region (800 μE m^{-2} s^{-1}). B, The response of i_T to step changes in light availability when held over a stomate in a white leaf region. Measured current decreases after the leaf is placed in the dark and increases after reillumination (800 μE m^{-2} s^{-1}). Measurements for A and B were made with a 7-μm-diameter carbon microelectrode.

sidiary cell membranes with the SECM. The flux of H^+ or K^+ from both cell types could then be examined in vivo with a potentiometric probe as the quantity and wavelength of the light varied. Guard and subsidiary cell responses to long-term (Field et al., 1995) and short-term (Mott, 1990) perturbations in CO_2 concentrations could be similarly explored. Longer term, we hope to develop a gas-phase scheme for measuring CO_2 and H_2O fluxes directly with SECM. Of course, the usefulness of SECM in examining in vivo cell physiology is not limited to studying stomata. SECM could be used to examine the regulation of other cell types that undergo reversible changes in turgor or those in which function depends on ion flux. Possibilities include pulvinal cells moving in response to light or circadian cycles (e.g. Schrempf et al., 1976; Björkmann and Prowles, 1981), floral cells regulating reversible opening and closing of flowers, and the selective absorption or exudation of compounds in localized root zones (e.g. Clarkson, 1985).

ACKNOWLEDGMENTS

We thank S. Assmann, S. Roux, J. Berry, and two anonymous reviewers for helpful comments on the manuscript. We also thank John Mendenhall and the Cell Research Institute at the University of Texas for assistance with the scanning electron microscopy image, and R.M. Brown for use of the fluorescence microscope.

Received June 24, 1996; accepted November 21, 1996.
Copyright Clearance Center: 0032–0889/97/113/0895/07.

LITERATURE CITED

Arca M, Bard AJ, Horrocks BR, Richards TC, Treichel DA (1994) Advances in scanning electrochemical microscopy. Analyst **119:** 719–726

Assmann S (1993) Signal transduction in guard cells. Annu Rev Cell Biol **9:** 345–375

Bard AJ, Fan FF, Pierce DT, Unwin PR, Wipf DO, Zhou F (1991) Chemical imaging of surfaces with the scanning electrochemical microscope. Science **254:** 68–74

Bard AJ, Fan FRF, Kwak J, Lev O (1989) Scanning electrochemical microscopy: introduction and principles. Anal Chem **61:** 132–138

Bard AJ, Faulkner LR (1980) Electrochemical Methods: Fundamentals and Applications. John Wiley & Sons, New York, p 145

Björkmann O, Prowles SB (1981) Leaf movement in the shade species *Oxalis oregana*. I. Response to light level and light quality. Carnegie Institution of Washington Year Book **80:** 59–62

Cardon ZG, Berry J (1992) Effects of O_2 and CO_2 concentration on the steady-state fluorescence yield of single guard cell pairs in intact leaf discs of *Tradescantia albiflora*. Plant Physiol **99:** 1238–1244

Clarkson DT (1985) Factors affecting mineral nutrient acquisition by plants. Annu Rev Plant Physiol **36:** 77–115

Dyar MT (1953) Studies on the reduction of a tetrazolium salt by green plant tissue. Am J Bot **40:** 20–25

Field CB, Jackson RB, Mooney HA (1995) Stomatal responses to, increased CO_2: implications from the plant to the global scale. Plant Cell Environ **18:** 1214–1225

Gautier H, Vavasseur A, Gans P, Lascève G (1991) Relationship between respiration and photosynthesis in guard cell and mesophyll cell protoplasts of *Commelina communis* L. Plant Physiol **95:** 636–641

Grantz DA, Graan T, Boyer JS (1985) Chloroplast function in guard cells of *Vicia faba* L. Measurement of the electrochromic absorbance change at 518 nm. Plant Physiol **77:** 956–962

Hansma PK, Drake B, Marti O, Gould SNC, Prater CB (1989) The scanning ion-conductance microscope. Science **243:** 641–643

Henriksen GH, Taylor AR, Brownlee C, Assmann SM (1996) Laser microsurgery of higher plant cell walls permits patch-clamp access. Plant Physiol **110:** 1063–1068

Horrocks BR, Mirkin MV, Bard AJ (1994) Application to investigation of the kinetics of heterogeneous electron transfer of semiconductor electrodes. J Phys Chem **98:** 9106–9114

Humble GD, Hsiao TC (1969) Specific requirement for potassium for light-activated opening of stomata in epidermal strips. Plant Physiol **44:** 230–234

Jackson RB, Woodrow IE, Mott KA (1991) Nonsteady-state photosynthesis following an increase in photon flux density (PFD): effects of magnitude and duration of initial PFD. Plant Physiol **95:** 498–503

Lee C, Kwak J, Bard AJ (1990) Application of scanning electrochemical microscopy to biological samples. Proc Natl Acad Sci USA **87:** 1740–1743

MacRobbie EAC (1987) Ionic relations of guard cells. *In* E Zeiger, GD Farquhar, IR Cowan, eds, Stomatal Function. Stanford University Press, Stanford, CA, pp 125–162

Melis A, Zeiger E (1982) Chlorophyll *a* fluorescence transients in mesophyll and guard cells. Plant Physiol **69:** 642–647

Mirkin MV, Arca M, Bard AJ (1992) Direct electrochemical measurements inside a 2000Å thick polymer film by scanning electrochemical microscopy. Science **257:** 364–366

Morris P, Linstead P, Thain JF (1981) Comparative studies of leaf tissue and isolated protoplasts. III. Effects of wall degrading enzymes and osmotic stress. J Exp Bot **32:** 801–811

Mott KA (1990) Sensing of atmospheric CO_2 by plants. Plant Cell Environ **13:** 731–737

Outlaw WH Jr, Mayne BC, Zenger VE, Manchester J (1981) Presence of both photosystems in guard cells of *Vicia faba* L. Implications for environmental signal processing. Plant Physiol **67:** 12–16

Reckmann U, Scheibe R, Raschke K (1990) Rubisco activity in guard cells compared with the solute requirement for stomatal opening. Plant Physiol **92:** 246–253

Schrempf M, Satter RL, Galston AW (1976) Potassium-linked chloride fluxes during rhythmic leaf movements of *Albizzia julibrissin*. Plant Physiol **58:** 190–192

Sestak Z, Catsky J, Jarvis PG (1971) Plant Photosynthetic Production: Manual of Methods. Junk, The Hague, The Netherlands

Shimazaki KI (1989) Ribulose bisphosphate carboxylase activity and photosynthetic O_2 evolution rate in *Vicia* guard-cell protoplasts. Plant Physiol **91:** 459–463

Shimazaki K-I, Gotow K, Kondo N (1982) Photosynthetic properties of guard cell protoplasts from *Vicia faba* L. Plant Cell Physiol **23:** 871–879

Shimazaki K-I, Zeiger E (1987) Red light-dependent CO_2 uptake and oxygen evolution in guard cell protoplasts of *Vicia faba* L. Evidence for photosynthetic CO_2 fixation. Plant Physiol **84:** 7–9

Wei C, Bard AJ (1995) Application of SECM to the study of charge transfer processes at the liquid/liquid interface. J Phys Chem **99:** 16033–16042

Wipf DO, Bard AJ (1991) Scanning electrochemical microscopy 7: effect of heterogeneous electron transfer rate at the substrate on the tip feedback. J Electrochem Soc **138:** 469–474

Wu W, Assmann SM (1993) Photosynthesis by guard cell chloroplasts of *Vicia faba* L.: effects of factors associated with stomatal movement. Plant Cell Physiol **34:** 1015–1022

Zeiger E, Armond P, Melis A (1980) Fluorescence properties of guard cell chloroplasts. Evidence for linear electron transport and light-harvesting pigments of photosystems I and II. Plant Physiol **67:** 17–20

Zeiger E, Farquhar GD, Cowan IR (1987) Stomatal Function. Stanford University Press, Stanford, CA